XPS studies of the $Zn_{1-x}Co_xS$ electronic structure

1994 J. Phys.: Condens. Matter 6 3369

(http://iopscience.iop.org/0953-8984/6/18/013)

J. Phys.: Condens. Matter 6 (1994) 3369–3378. Printed in the UK

XPS studies of the $Zn_{1-x}Co_xS$ electronic structure

K Ławniczak-Jabłońska†, Z Gołacki†, W Paszkowicz†, J Mašek‡, L-S Johansson§ and M Heinonen§

† Institute of Physics, Polish Academy of Sciences, Aleja Lotnikow 32/46, 02 668 Warszawa, Poland

‡ Institute of Physics, Czech Academy of Sciences, Na Slovance 2, CZ-18040 Praha 8, Czech Republic

§ Department of Applied Physics, University of Turku, ElectroCity, Tykistokatu 2D, SF-20520 Turku, Finland

Received 12 January 1994

Abstract. We have investigated electronic states of diluted magnetic semiconducting $Zn_{1-x}Co_xS$ compounds, using x-ray photoelectron spectroscopy (XPS). The amount of Co substituting Zn in the ZnS lattice was in the range $0 < x < 0.25$. In order to evaluate the influence of Co on the electronic structure of these compounds, XPS spectra of both the core states and the valence band were analysed.

We found that the addition of Co into the ZnS lattice did not affect the Zn 2p core levels but that in these alloys the S 2p doublets were split into two components, with a binding energy difference of 0.3 eV. The intensity ratio of the two S 2p components followed the changes in the Zn–Co ratio of the alloys. The binding energy of Co 2p core levels in the alloys was similar to that in CoO, indicating the similarity between the ionic strength (+2) of the Co–S and Co–O bonds.

The valence band spectra revealed a significant contribution of Co 3d electrons to the density of states (DOS). The valence band DOS distribution was also calculated from theory, using a tight-binding version of the coherent potential approximation. According to the calculations, an increase in the Co content of the alloy should cause changes in the valence band DOS similar to those observed from the x-ray photoelectron spectra.

1. Introduction

The diluted magnetic semiconducting (DMS) alloys are solid solutions of non-magnetic semiconducting compounds containing an appreciable number of transition or rare earth metal ions with magnetic moment. The partial substitution of a cation by a magnetic ion results in hybridization of the 3d or 4f states with the sp band states of host semiconductors (see, e.g., [1] and [2]). This inevitably leads to modification in the crystal and electronic structure [3, 4]. For over two decades numerous research projects have been concentrated on the Mn-based II–VI DMS alloys. Mn-doped compounds exhibit interesting magnetic, transport and optical properties including bound magnetic polarons, spin glasses, cluster antiferromagnetism and pronounced magneto-optical effects [5–7]. These properties are thought to arise from the combination of localized Mn 3d and sp-like states of the host.

The degree of hybridization of the Mn 3d states and their interaction with the host band states have been a subject of many discussions (see, e.g., [8] and [9]). However, the photoemission spectra revealed both a strong hybridization of the Mn 3d(t) with the host anion p band states and the localized nature of the Mn 3d(e) states with a maximum located

0953-8984/94/183369+10$19.50

at about −3.5 eV from the valence band edge [8, 10]. This has been confirmed furthermore by several density of states (DOS) calculations [9, 11, 12].

During recent years the widespread scientific interest in DMS alloys included also the II–VI materials with Fe and Co [13, 14]. The DMS alloys based on Co have properties similar to their Mn-based counterparts, except that their magnetic moments are smaller, due to the different filling of the d shells. It has been reported that the exchange interaction of the magnetic moment in Co-based DMS alloys is several times larger than that of the systems with Mn [15, 16].

Up to now there have been only a few experimental or theoretical investigations on the electronic structure of these materials [17, 18]. The calculations performed by Mašek [18] have confirmed the observed increase in the exchange interaction between Co magnetic moments for the $Zn_{1-x}Co_xSe$ DMS alloy. This was explained by the difference in the distribution of the d states in valence bands of the Co- and Mn-based DMS alloys.

These interesting phenomena stimulated us to perform the systematic investigation of the DMS alloy $Zn_{1-x}Co_xS$. The x-ray photoelectron spectroscopy (XPS) studies were supported by x-ray diffraction and electron probe micro-analysis (EPMA) of the samples to avoid discrepancies between nominal and real content of Co.

2. Experimental details

The $Zn_{1-x}Co_xS$ specimens were grown by chemical vapour transport using I as a transport agent. The chemical composition of the crystals was determined by EPMA, using a Jeol JSM-50A. According to these results, the Co content of the five samples reported here was $x = 0.03$, 0.05, 0.12, 0.20 and 0.25. The x-ray diffraction studies performed with a conventional x-ray powder diffractometer (Cu Kα radiation) confirmed that all the samples reveal zinc blende structure. The diffractograms showed no traces of another phase. For the selected single-crystal grains (about 5 mm in diameter) the lattice constant was determined by the Bond method using a high-resolution diffractometer equipped with two channel-cut monochromatizing Ge crystals employing 220 reflection and Cu Kα_1 radiation. The absolute lattice constant value was calibrated using a reference Si single crystal. According to these results, the lattice constants of the investigated crystals were found to be linearly dependent on the Co content x, as known from the literature [19, 20] (figure 1). Detailed results of x-ray investigations will be published elsewhere [21].

The XPS spectra were recorded with a Perkin–Elmer 5400 small-spot ESCA spectrometer equipped with a hemispherical analyser. Each specimen was cleaved *in situ* in UHV prior to the measurement in order to obtain a clean surface. Since the ZnS and $Zn_{1-x}Co_xS$ pseudo-binary compounds have a low conductivity, the calibration of the energy scale was a significant problem, due to sample charging effects. This was compensated by measuring each sample in two different excitation modes, namely by using non-monochromatized Mg Kα (1253.6 eV) radiation (mode 1) or Al Kα (1486.6 eV) radiation with a Rowland circle monochromator (mode 2).

In mode 1 the measurements were performed using 17.9 analyser pass energy and 0.1 eV step. The charging effects were minimized by lowering the x-ray tube to within 1 cm from the sample surface: during the measurement the secondary electrons excited from the Al window of the x-ray tube neutralized the sample surface. With this mode either no surface charging was detected or the surface charging resulted only in a constant shift in the binding energy scale, which was corrected using the adventitious C 1s line as in [22].

In mode 2 the measurements were performed using 17.9 eV or 8.95 eV analyser pass energy. With this mode, a slightly non-linear change in the binding energy scale was

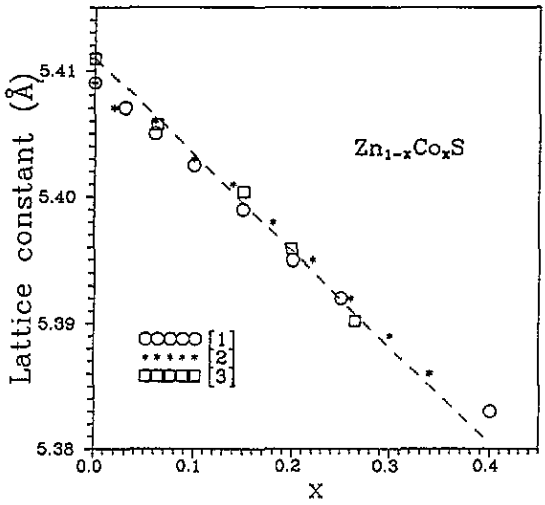

Figure 1. The lattice constant as a function of mole fraction, x, in $Zn_{1-x}Co_xS$: 1, powder data of Niu *et al* [19]; 2, powder data of Becker and Lutz [20]; 3, single-crystal data of this work.

detected due to charging effects. This was caused by either complex discharging processes [23] or backscattering of emitted electrons [24]. This surface charging was neutralized using a low-energy electron bombardment of the crystal surface during the measurement. The width of the Zn 2p line turned out to be very sensitive to charging, which allowed us to check whether the neutralization current was satisfactory.

3. Theory

The photoemission valence band spectrum from a disordered mixed crystal is closely related to the configurationally averaged density of states (DOS). In particular, the spectrum can be obtained as a sum of partial DOSs, decomposed according to atomic orbital momenta, weighted by the appropriate transition matrix elements and convoluted with broadening functions.

To calculate the electronic structure of a diluted magnetic semiconductor in its paramagnetic state, one has to consider the combined effects of electron correlation, hybridization and disorder. We proceed by using a simple tight-binding version of the spin fluctuation theory [25–27].

We start with a many-body Hamiltonian

$$H = H_{\text{band}} + H_{\text{imp}} + H_{\text{int}}$$

the three parts of which correspond to the motion of the electrons in bands, to their scattering at the transition metal impurities, and to their mutual interactions, respectively.

The band structure of the host semiconductor crystal with a zinc blende structure is represented by a tight-binding Hamiltonian with cationic d states added to the usual sp^3 basis (for details see [27]).

The change of the crystal potential due to the substitution of Co is represented by a shift of the atomic s and d levels at the sites where the substitution takes place. The shift

is particularly important for the d states, which are in this way transferred from the core region into the valence band. The electron–electron interaction is restricted only to the Co 3d states. The coupling within each d shell is described by a multiband Anderson–Parmenter Hamiltonian, which takes into account both the Coulomb repulsion of the d electrons and the exchange interaction. In the sense of the spin fluctuation theory [25], the unrestricted Hartree–Fock approximation is applied to each Co site separately. The electron–electron interaction results then in an exchange splitting of the Co d levels. These splittings, only weakly affected by the hybridization with the overlapping bands, stabilize the maximum total spin $\frac{3}{2}$ of the ion according to the Hund's rule. The orientation of the magnetic moment at each site is, however, random in the paramagnetic state, and varies with time. This magnetic disorder is, as usual, treated in the static limit, and only two opposite directions, up and down, are allowed for the magnetic moment orientation.

With these limitations, we obtain an effective quasi-ternary mixed crystal $Zn_{1-x}Co_{\uparrow,x/2}Co_{\downarrow,x/2}S$ representing the paramagnetic state of $Zn_{1-x}Co_xS$. Both chemical and magnetic disorder (originating from the many-electron correlation) can be then treated on the same basis by using the coherent potential approximation (CPA) [28]. The results of the calculations are presented in figures 2 and 3. In figure 2 the states symmetry and site projected are shown for samples with $x = 0.12$ whereas in figure 3 the total DOSs for all samples considered are presented.

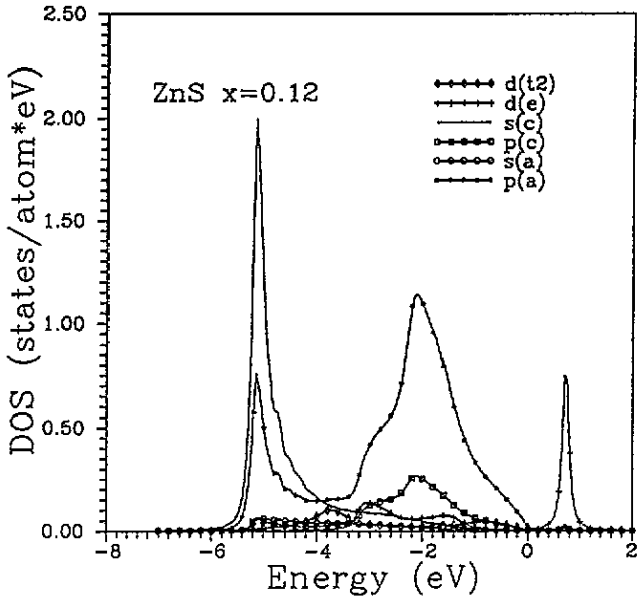

Figure 2. DOS symmetry and site projected for $Zn_{1-x}Co_xS$ samples with $x = 0.12$. 'c' denotes cation states, 'a', anion states and, 'e' and 't_2', different symmetries of the d orbital.

It is important to note that the Co ions with seven d electrons differ from the well known case of Mn. In Mn with a half-filled d shell the exchange splitting is the same for all orbitals. In Co, the sub-shells with orbital symmetry t and e must be treated separately, and the resulting atomic potential is characterized by four effective atomic levels $e_{t,\uparrow}$, $e_{t,\downarrow}$, $e_{e,\uparrow}$ and $e_{e,\downarrow}$. Clearly, the exchange splitting of the states with the e symmetry, which are occupied by electron pairs, is less than the splitting for the singly occupied t_2 states, and this effect puts $e_{e,\downarrow}$ just above the valence band top [18,27].

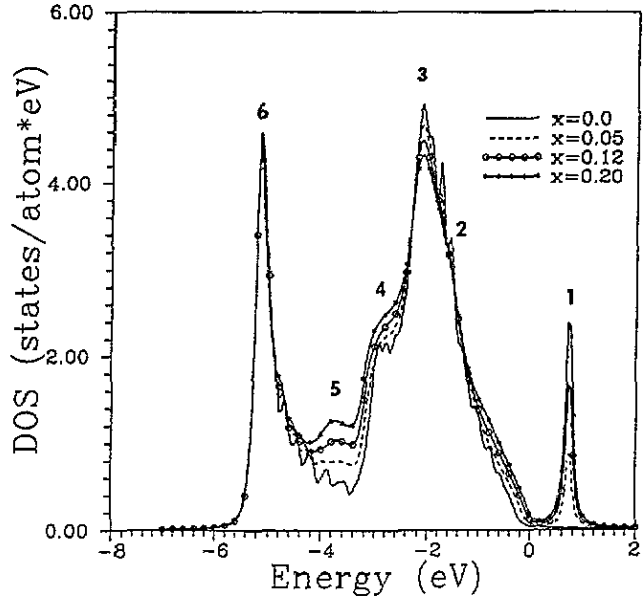

Figure 3. The total DOS energy distribution for $Zn_{1-x}Co_xS$ with different x. The distribution features indexed here and in the following figures by numbers 1–6 are discussed in the text.

4. Results and discussion

To estimate the changes in the electronic structure of ZnS produced by the substitution of Zn cations with Co ions both the Zn 2p, Co 2p, and S 2p core lines and the valence band spectra of the pure ZnS and $Zn_{1-x}Co_xS$ compounds were recorded under the same experimental conditions. The precise investigation of the energy positions and the peak shape showed that the introduction of Co into a ZnS lattice did not affect the binding energy or the peak shape of the Zn 2p doublet (within experimental accuracy) in the composition range of $x \leqslant 0.25$. This indicates that the Zn–S bond length in the crystals studied remained unchanged, just as e.g. in the case of the Cd–Te bond in the $Cd_{1-x}Mn_xTe$ alloys [4].

The Co 2p line was detected in the XPS spectra for all the samples studied, including the one with the lowest Co content, namely $x = 0.03$ (figure 4). The Co 2p lines were shifted 2 eV from that of elemental Co [40]. The binding energies of Co $2p_{3/2}$ (780 eV) and Co $2p_{1/2}$ (795 eV) core levels were found to be constant throughout the composition range of $x < 0.25$. The shift indicates the similarity between the ionic strength (+2) of the Co–S and Co–O bonds [29].

Changes in the shape of the S 2p core line (figure 5) are caused by the substitution of Zn by Co, which leads to a gradual change of the S near neighbours (S–Zn, S–Co). Assuming a random substitution of Zn atoms by Co atoms in the cationic sublattice, the observed changes can be ascribed to the differences in binding energies of the S 2p electrons in S atoms having a Co neighbour or not. The results of an EXAFS investigation on Co–S and Zn–S bond lengths showed [30] that the lengths of these bonds were 2.315 Å and 2.344 Å, respectively, independent of the compositional changes in the alloy. This suggests the bond strength of Co–S to be larger than that of Zn–S, and thus the 2p electrons of S atoms bonded with Co should be shifted towards higher binding energies.

In order to decompose the S 2p peak, a curve fitting procedure was applied by using a pseudo-Voigt function [31] for each component, resulting in two doublets (figure 6). The

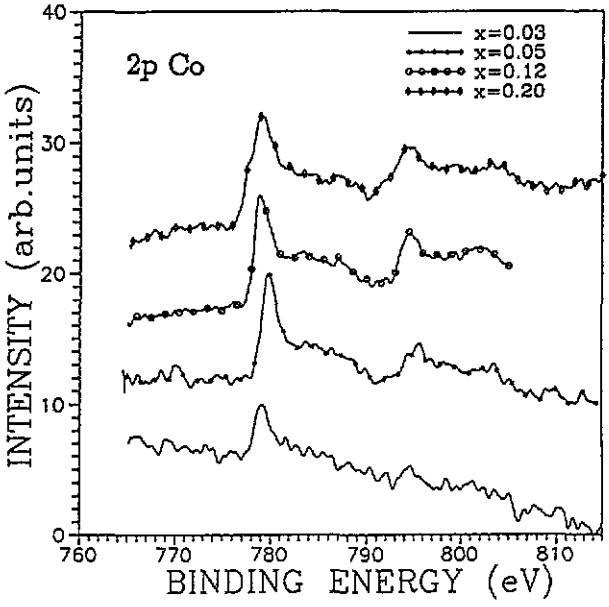

Figure 4. The XPS spectra of Co 2p line as registered for $Zn_{1-x}Co_xS$ samples with different x.

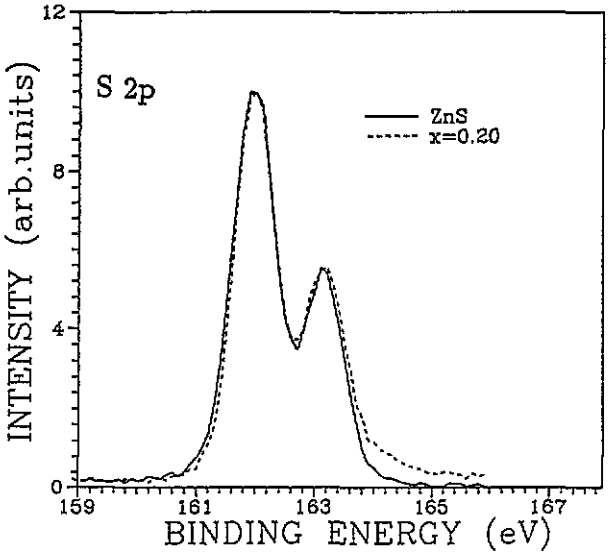

Figure 5. The XPS spectra of the S 2p line for ZnS and $Zn_{1-x}Co_xS$ with $x = 0.20$.

Voigt or pseudo-Voigt line shape representing mixed Gaussian/Lorentzian profiles [32, 33] is appropriate for XPS peaks measured for clean semiconductor surfaces [32]. The Lorentzian contribution of these functions describes the natural line width and core hole lifetime, while the Gaussian contribution represents the instrument response function and the phonon broadening of the core level [32]. The S 2p peaks measured from $Zn_{1-x}Co_xS$ specimens were fitted with a line width equal to that measured for ZnS. The mixing parameter of the

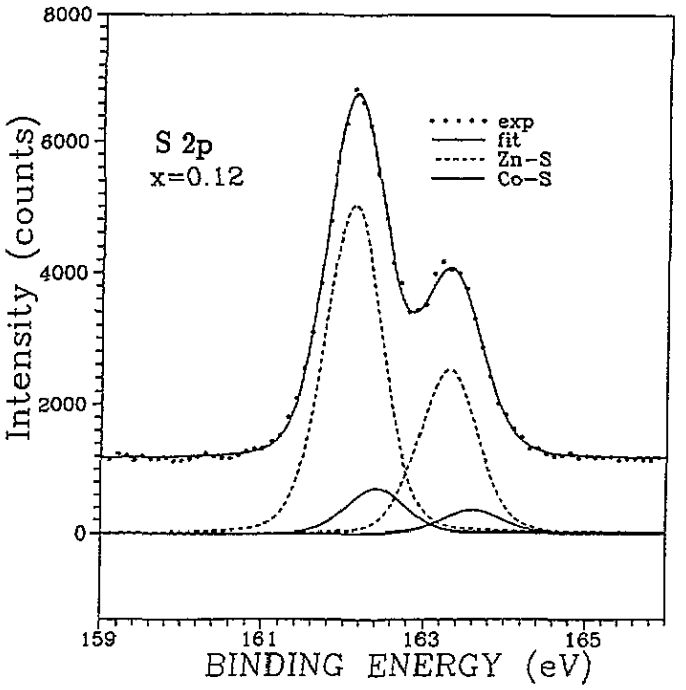

Figure 6. The XPS spectrum of the S 2p line for $Zn_{1-x}Co_xS$ with $x = 0.12$. The solid line approximation of the experimental points is a result of a peak profile fitting procedure using the pseudo-Voigt profile function. The dashed line denotes the 2p orbital doublet of the Zn-coordinated S atom; the solid line refers to the same S 2p orbital coordinated with three Zn atoms and one Co atom.

pseudo-Voigt function was treated as a free one.

According to the results of the fitting procedure, the position of the second S 2p doublet was shifted by 0.3 eV towards higher binding energy from that observed in the pure ZnS. The second doublet was ascribed as representing the fraction of S 2p electrons from S atoms bonded with one Co and three Zn atoms. The intensity of the second doublet followed the composition of samples. However, for the samples with $x = 0.20$ and 0.25 the two-doublet fit was not as good as that for $x = 0.12$. The expected source of the discrepancy would be the presence of a third component that is related to the atoms of S bonded with two Co and two Zn atoms. The probability of such coordinations increases with increasing Co content [34].

Figure 7 gives the XPS spectra of the valence band (VB) recorded for $Zn_{1-x}Co_xS$ DMS alloys with composition ranging from pure ZnS up to $x = 0.25$. For better comparison, the spectra were normalized to the maximum height. The VB structure was found to depend significantly on the Co content, showing the contribution of Co 3d electrons to the VB DOS of ZnS. An increase of the Co content induced additional spectral features (marked '1' and '2') in the vicinity of the top of the VB, which leads to broadening of the VB by almost 1 eV.

The identification of the distribution of states in the VB was made using the calculated DOS (figure 3) which shows all characteristic features observed in the XPS VB spectra.

In figure 2 the local and partial components from the DOS calculation are presented for $x = 0.12$ as an example. The comparison with the experimental spectra allowed us to assign

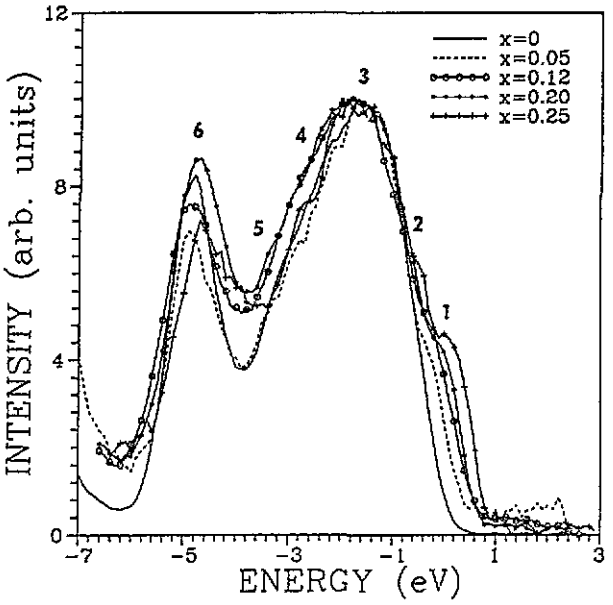

Figure 7. The XPS spectra of the valence band for ZnS and $Zn_{1-x}Co_xS$ with $x = 0.05$, 0.12, 0.20, and 0.25.

a given structure in the spectra to its dominating orbital origin. The pronounced structure marked '1' results from the spin-down d states of Co. Notice that this structure, not present in Mn-based DMS alloys, is a unique feature of Co-containing DMS alloys [18, 35]. These states, which have a d(e) symmetry and are not much hybridized with the VB states of the host material, are localized just above the VB top of the host material. It is worth emphasizing that this is the first experimental evidence of the Co-related DOS found in the energy gap of ZnS due to the formation of a pseudobinary DMS compound, whereas the impurity-limited case of ZnS:Co is known in the literature (see, e.g., [36]). In our experimental spectra this peak is not separated from the VB, in contrast with the calculations. Also, UPS measurements of these alloys, which provide better energy resolution, have not shown any separation [37].

The structure marked '2' is formed predominantly by p states of S with addition of the $d(t_2)$ Co states. At the maximum '3' located at about -2 eV, the p states of Zn and S atoms dominate. In the valley between maxima '3' and '6' the Co states are seen again. At the structure marked '4' the d(e) states dominate whereas at the structure '5' the $d(t_2)$ states do. Maximum '6' is formed of s states of Zn and p states of S. The photoionization cross section for these states is much lower than that for d states of Co, thus explaining the decrease in observed intensity as compared to the DOS calculation.

In figure 8(*a*) the DOSs weighted by the Scofield photoionization cross section (M) [38] for Al Kα radiation are shown. Furthermore in figure 8(*b*) the weighted DOSs are convoluted with two broadening functions. A Gaussian with FWHM = 0.7 eV accounts for the experimental broadening of spectra and a Lorentzian with FWHM $= 0.3 + 0.1E$ (where E is the energy in electronvolts) accounts for the lifetime of the VB hole. The dependence of the hole life time on the energy position in the VB is taken into account by the E dependence of the Lorentzian FWHM [39]. Despite the non-identical intensity distribution in the calculated and measured spectra, all changes with the content of Co observed in the experiment were reproduced also in the calculated spectra. The only remarkable difference

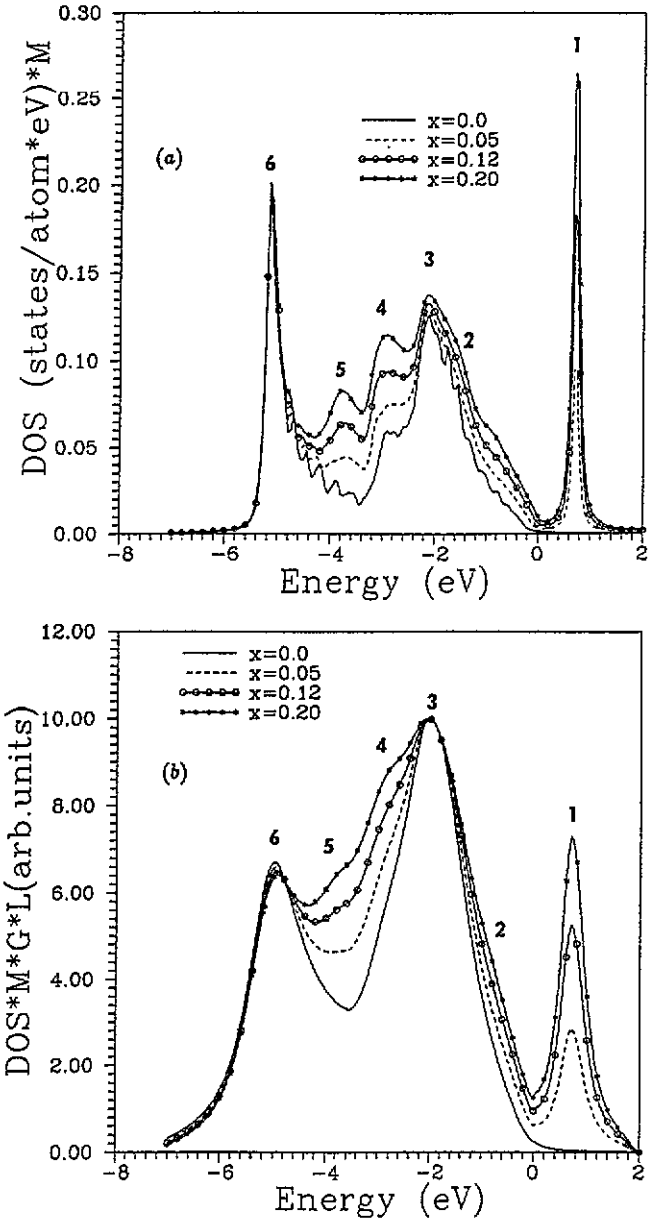

Figure 8. (*a*) The DOS weighted by the Scofield photoionization cross section, M, for Al Kα-radiation. (*b*) The DOS weighted by the Scofield photoionization cross section, M convoluted with a Gaussian (G) with FWHM = 0.7 eV and a Lorentzian (L) with FWHM = $0.3+0.1E$, where E is the energy in electronvolts.

is the dip between the VB and Co d(e) states above it in the theoretical DOS. We expect that this dip would disappear in a more realistic calculation in which many-body effects in the Co d shells are considered more carefully. Also the structural disorder (different Zn–S and Co–S distances) acting on the S p states may influence the VB top.

Acknowledgments

This work was supported (in part) by the State Committee for Scientific Research, under grant No 2 2314 9102 and by the Finnish Academy of Sciences. The authors are indebted to Dr R Iwanowski for fruitful discussions.

References

[1] Fujimori A 1991 *Diluted Magnetic Semiconductors* ed M Jain (Singapore: World Scientific) p 117 and references therein
[2] Furdyna J K 1988 *J. Appl. Phys.* **64** R29
[3] Jain M and Robins J L 1991 *Diluted Magnetic Semiconductors* ed M Jain (Singapore: World Scientific) p 1
[4] Balzarotti A, Czyżyk M, Kisiel A, Motta N, Podgorny M and Zimnal-Starnawska M 1984 *Phys. Rev.* B **30** 2295
[5] Heiman D, Wolff P A and Warnock J 1983 *Phys. Rev.* B **28** 4848
[6] Gałazka R R, Nagata S and Keesom P H 1980 *Phys. Rev.* B **22** 3344
[7] Gaj J A, Planel R and Fishman G 1979 *Solid State Commun.* **29** 435
[8] Taniguchi M, Ley L, Johnson R L, Ghijsen J and Cardona M 1986 *Phys. Rev.* B **33** 1206
[9] Wei S-H and Zunger A 1987 *Phys. Rev.* B **35** 2340
[10] Orłowski B A, Kopalko K and Chab W 1984 *Solid State Commun.* **50** 749
[11] Podgorny M 1988 *Z. Phys.* B **69** 501
[12] Larson B E, Hass K C, Ehrenreich H and Carlsson A E 1985 *Solid State Commun.* **56** 347
[13] Twardowski A 1990 *J. Appl. Phys.* **67** 5108
[14] Shapira Y 1991 *Semimagnetic Semiconductors and Diluted Magnetic Semiconductors* ed M Averous and M Balkanski (New York: Plenum) p 121
[15] Lewicki A, Schindler A I, Furdyna J K and Giriat W 1989 *Phys. Rev.* B **40** 2379
[16] Lewicki A, Schindler A I, Miotkowski I and Furdyna J K 1990 *Phys. Rev.* B **41** 4653
[17] Orłowski B A, Kowalski B J and Chab V 1990 *Phys. Scr.* **41** 984
[18] Mašek J 1991 *Solid State Commun.* **78** 351
[19] Niu C-M, Kershaw R, Dwight K and Wold A J 1990 *Solid State Chem.* **85** 262
[20] Becker W and Lutz H D 1978 *Mater. Res. Bull.* **13** 907
[21] Paszkowicz W, Domagala J and Golacki Z to be published
[22] Swift P 1982 *Surf. Interface Anal.* **4** 47
[23] Cazaux J and Lehuede P 1992 *J. Electron Spectrosc. Relat. Phenom.* **59** 49
[24] Barth G, Linder R and Bryson C 1988 *Surf. Interface Anal.* **11** 307
[25] Moriya T 1985 *Spin Fluctuations in Itinerant Electron Magnetism* (Berlin: Springer)
[26] Mašek J, Velicky B and Janiš V 1987 *J. Phys. C: Solid State Phys.* **20** 59
[27] Mašek J to be published
[28] Velicky B, Kirkpatrick S and Ehrenreich H 1968 *Phys. Rev.* **175** 747
[29] Kim K S 1975 *Phys. Rev.* B **11** 2177
[30] Ławniczak-Jabłońska K and Gołacki Z *Acta Phys. Pol.* submitted
[31] Wertheim G K, Butler M A, West K W and Buchanan D N E 1974 *Rev. Sci. Instrum.* **45** 1369
[32] Joyce J J, del Giudice M and Weaver J H 1989 *J. Electron Spectrosc. Relat. Phenom.* **49** 31
[33] Evans S 1991 *Surf. Interface Anal.* **17** 85
[34] Balzarotti A, Motta N, Kisiel A, Zimnal-Starnawska M, Czyzyk M T and Podgorny M 1985 *Phys. Rev.* B **31** 7526
[35] Mašek J 1991 *Acta Phys. Pol.* A **80** 267
[36] Vogl P and Baranowski J M 1985 *Acta Phys. Pol.* A **67** 133
[37] Kowalski B J, Gołacki Z, Guziewicz E, Orłowski B A, Mašek, Ghijsen J, Johnson R *Acta Phys. Pol.* submitted
[38] Scofield J H 1976 *J. Electron Spectrosc. Relat. Phenom.* **8** 129
[39] Muller J E, Jepsen O and Wilkins J W 1982 *Solid State Commun.* **42** 365
[40] Lebugle A, Axelsson U, Nyholm R and Martesson N 1981 *Phys. Scr.* **23** 825